Geotechnical Engineering for the Preservation of Monuments and Historic Sites III – Lancellotta, Viggiani, Flora, de Silva & Mele (Eds)

Influence of soil deposit heterogeneity on the dynamic behaviour of masonry towers

A.F. D'Oria, G. Elia, A. di Lernia & G. Uva
Department of Civil, Environmental, Land, Building Engineering and Chemistry (DICATECh), Technical University of Bari, Bari, Italy

ABSTRACT: The paper deals with the direct soil-structure interaction numerical modelling of an ideal masonry tower resting on deformable heterogeneous soil deposits. The stratigraphic heterogeneity is modelled dividing each deposit into several layers to implement four different shear wave velocity profiles. The resulting deposits can be classified as class C according to the Italian seismic building code prescriptions. Complete three-dimensional finite element dynamic analyses are carried out assuming a visco-elastic behaviour for both the tower and the soil, with the aim to investigate the effects of the soil heterogeneity on the dynamic response of the structure in the elastic field. Practical relationships are derived from the results to predict the deviation of the tower dynamic behaviour from a fixed-base condition.

1 INTRODUCTION

The response of a structure during a seismic event is the result of the mutual interaction between the structure itself, the supporting foundation and the surrounding soil, which is usually known as dynamic soil-structure interaction (SSI). Commonly, two methods are adopted to study the SSI problem: i) the substructure approach, which consists in decoupling the full system into the three constitutive parts to be separately analysed and ii) the direct approach, which consists in a single fully coupled analysis of the whole soil-structure system. The direct approach, especially if combined with a three-dimensional numerical model, should generally ensure more accurate and reliable solutions as the complexity of the problem increases (Amorosi et al. 2017; Casciati & Borja 2004; di Lernia et al. 2019; Torabi & Rayhani 2014).

Historical structures are typically characterized by a huge level of complexity in terms of geometry, materials properties, loads and boundary conditions which need to be modelled in order to correctly represent the reality. In this context, masonry towers, in the form of medieval defense structures as well as bell towers in churches, represent an important part of the historical and architectural heritage to be preserved. These structures are particularly sensitive to damage and prone to partial or even total collapse under seismic actions due to their material characteristics and geometric configurations. Several studies have been recently carried out to assess the performance of masonry towers investigating, with various approaches, the effects of the critical aspects controlling their dynamic response, such as the geometric irregularities, inclination, material properties and input motion characteristics.

However, very often the structure is assumed to be perfectly fixed at the base (Bartoli et al. 2016; Castellazzi et al. 2018; Clementi et al. 2019; Milani 2019; Sarhosis 2018; Valente & Milani 2016, 2018), thus neglecting the effect of the soil deformability which can considerably modify its structural dynamic behaviour. Indeed, the few studies available in the literature accounting for this effect (Casolo & Uva 2013; de Silva et al. 2018a, b; de Silva 2020; Casolo et al. 2017; Mortezaei & Motaghi 2016) indicate that the soil compliance can cause i) the elongation of the natural periods of the masonry structure and ii) a deviation from the cantilever modal shape especially from the

 DOI 10.1201/9781003308867-59

second vibration mode onwards, which can cause relevant alterations in the loading distribution along the tower. Nevertheless, a homogeneous deposit is usually modelled at the base of the tower, thus rarely considering a realistic stratigraphic soil profile, with the exception of very few cases (e.g. de Silva et al. 2018a, b).

This study focuses on investigating the dynamic response of an ideal masonry tower resting on different heterogeneous soil deposits by means of direct SSI analyses performed assuming a visco-elastic behaviour for both the structure and the soil, starting from the work by Casolo et al. (2017) in which two homogeneous soil deposits were considered. The geometrical and mechanical properties of the ideal tower and the soil profiles are firstly described in Section 2. Then, a preliminary validation analysis of the wave propagation process through the soil deposits in free-field conditions is presented in Section 3. Finally, the impact of the soil heterogeneity on the tower seismic response is investigated by conducting 3D SSI dynamic simulations, highlighting its deviation from the typical cantilever condition.

2 CASE STUDIES AND MODELS ADOPTED

Four ideal soil deposits have been selected to be representative of real possible stratigraphies along the Italian territory. The upper and the lower bound V_S profiles with depth used by Falcone et al. (2021) to describe the typical lithological successions of clay and sand cover soils in Italy have been considered as the reference range within which the four V_S profiles have been build up. Each deposit is 30m deep and is divided in 5m thick layers, with the exception of the top two strata which have a thickness of 2.5m. The four profiles, shown in Figure 1, share the same value of the equivalent shear wave velocity ($V_{S,eq}$), equal to 250m/s, so that they can be classified as class C deposits ($180<V_{S,eq}<360$m/s) according to the Italian Code NTC 2018 (Consiglio dei Ministri 2018). The $V_{S,eq}$ is defined by:

$$V_{S,eq} = \frac{H}{\sum_{i=1}^{N} \frac{h_i}{V_{S,i}}} \tag{1}$$

where N is the number of the layers, h_i is the thickness of the i-th layer, $V_{S,i}$ is the shear wave velocity in the i-th layer, while H is the deposit depth.

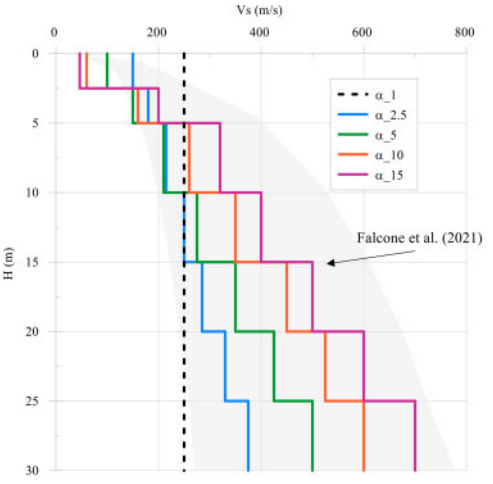

Figure 1. Soil profiles selected within the range defined by Falcone et al. (2021).

The soil profiles are characterized by different values of V_S at the top (V_0) and at the bottom (V_H) of the deposit, resulting in four ratios $\alpha=V_H/V_0$ equal to 2.5, 5, 10 and 15, with the aim to cover a wide range of heterogeneity cases with respect to the homogeneous condition (i.e. $\alpha=1$).

Following the work by Casolo et al. (2017), the investigated masonry tower represents an ideal case study, covering the main features of many recurring bell towers located in the seismic areas of Northern Italy. Its dimensions and mechanical properties were chosen by analysing a series of representative examples available in the literature and are summarized in Table 1.

Table 1. Geometrical features and mechanical properties of the tower.

Height (m)	Section (m)	Foundation (m)	ρ (kg/m^3)	E (MPa)	ν (–)
27	5.3 × 5.3	6.8 × 6.8 × 2.5	1900	3500	0.1

The tower is supposed to be structurally independent from other buildings and is characterized by a quite simplified and regular geometric configuration both in plan and in elevation (Figure 2a). The structure is 27m high, has a section of 5.3 × 5.3m^2 and a larger square foundation (6.8 × 6.8m^2) with a thickness of 2.5m.

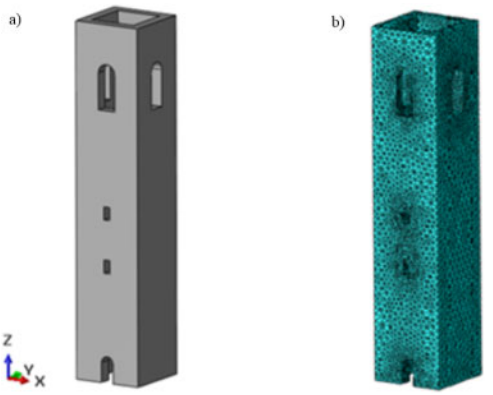

Figure 2. a) 3D masonry tower and b) FEM model (modified after Casolo et al. 2017).

The masonry tower has been modelled in 3D using the 4-node linear tetrahedral elements (C3D4) available in the finite element (FE) software ABAQUS (2014). The mesh, shown in Figure 2b, consists of 15471 nodes and it has been refined around the openings and near the foundations to achieve a high numerical accuracy. A linear-elastic constitutive law has been adopted in the simulations, using the properties reported in Table 1.

With the aim of validating the 3D numerical approach in simulating the free field seismic ground response, results obtained by 3D numerical scheme have been compared to those achieved through the 2D scheme. The 2D model has been discretized using 4-node bilinear plane-strain elements with reduced integration (CPE4R) (Figure 3a), while C3D4 elements have been adopted for the 3D discretization (Figure 3b). In both cases, the coarseness of the FE mesh has been refined in order to obtain a distance between two consecutive nodes smaller than approximately one-eighth of the wavelength associated with the maximum frequency content of the input motion (Bathe 1996; Kuhlemeyer & Lysmer 1973), equal to 15Hz. Tied-nodes boundary conditions have been reproduced on the vertical sides of the soil models to allow for a one-dimensional wave propagation: the nodes at the same depth along the lateral boundaries have been constrained to move horizontally by the same quantity, while their vertical displacements have been forbidden. The nodes at bottom

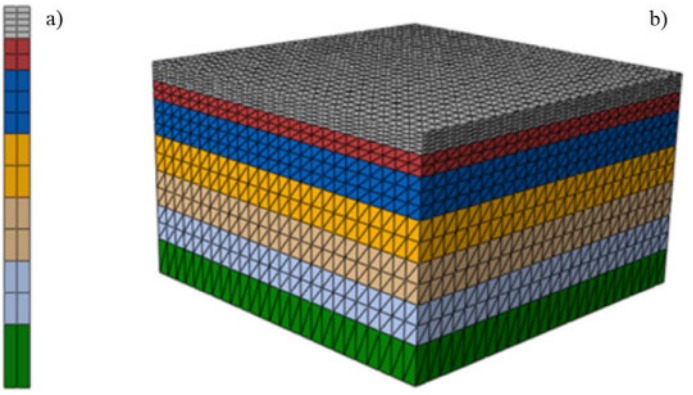

Figure 3. a) 2D and b) 3D FE models of the heterogeneous soil deposits.

have been fixed to simulate a rigid bedrock, while the presence of water in the deposit has been neglected.

The employed 2D models are characterized by a width equal to 2m, while the 3D models, which should accommodate the tower on the top, have a wider extension along the two horizontal directions (i.e. 50m), as indicated by a preliminary sensitive analysis. To introduce the stratigraphic heterogeneity, the Young modulus corresponding to the V_S values described in Figure 1 has been assigned to each soil layer, assuming a Poisson's coefficient equal to 0.2 and a material density of 1800kg/m^3. The dissipative capacity of the soil has been introduced by the frequency-dependent viscous damping Rayleigh formulation (Clough & Penzien 1993), in which the damping matrix [C] is a linear combination of the mass [M] and stiffness [K] matrices of the system:

$$[C] = \alpha_R[M] + \beta_R[K] \tag{2}$$

The Rayleigh coefficients α_R and β_R are derived as a function of the target damping ratio D according to Eq. 3:

$$\begin{Bmatrix} \alpha_R \\ \beta_R \end{Bmatrix} = \frac{2D}{\omega_m + \omega_n} \begin{Bmatrix} \omega_m & \omega_n \\ 1 & \end{Bmatrix} \tag{3}$$

The angular frequencies ω_m and ω_n are related to the frequencies f_m and f_n, defining the interval over which the viscous damping is equal to or lower than the target damping ratio D, assumed herein equal to 5% for each soil layer. The selection of the two frequencies requires a suitable calibration strategy, as proposed, for example, by Amorosi et al. (2010). In this particular case, the two Rayleigh frequencies have been set equal to the first and second natural frequencies of the soil deposit. Indeed, preliminary modal eigenvalue analyses of the soil-structure interaction problem indicated that the dynamic behaviour of the tower is particularly influenced by the second natural mode of the soil deposit, which confirm the results presented by Casolo et al. (2017). In addition, a 5% Rayleigh damping has also been added to the linear-elastic model describing the masonry behaviour, calibrated considering the first and second vibration mode of the structure. Therefore, the tower and the soil deposit have been considered as visco-elastic materials, neglecting the nonlinear effects induced by the seismic action during the FE simulations.

The dynamic analyses have been conducted in ABAQUS using the unconditionally stable implicit Hilber-Hughes-Taylor time integration scheme, i.e. an extension of the Newmark β-method, which ensures the stability of the algorithm without introducing any additional numerical damping. The reference input motion employed in the numerical simulations is represented by the north-south component recorded by the station MIR02, located in Mirandola (MO), during the 2012 Emilia-Romagna main earthquake event. Its time history and Fourier spectrum are shown in Figure 4. The

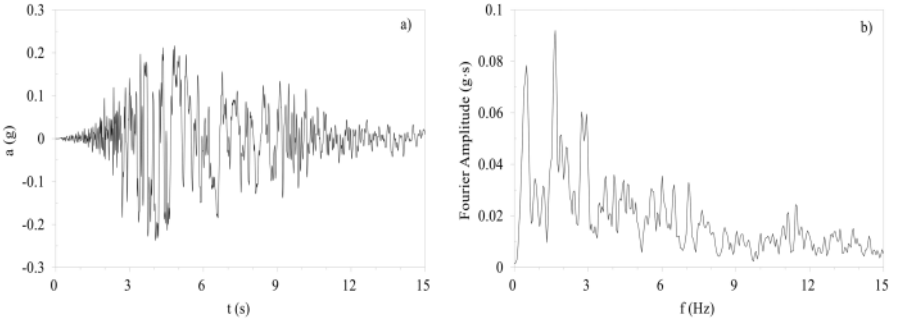

Figure 4. Mirandola earthquake: a) acceleration time history and b) Fourier spectrum.

seismic signal is characterized by a maximum acceleration of 0.22g, a time step equal to 0.005s, while its total length has been reduced to just 15s.

3 RESULTS

A first set of dynamic simulations conducted with ABAQUS in 2D and 3D are first presented to validate the results of the free-field wave propagation process in heterogeneous soil deposits against the corresponding 1D output obtained through a linear visco-elastic approach performed with the equivalent-linear visco-elastic code EERA (Bardet et al. 2000). This allows to check the reliability of the ABAQUS results from a geotechnical point of view. Then, the dynamic SSI analyses of the ideal masonry tower resting on the four heterogeneous deposits are presented and commented.

3.1 *EERA analyses*

The four V_S soil profiles described in Section 2 have been implemented in EERA, assuming a rigid bedrock and a constant damping ratio equal to 5% along the column depth. The soil has been considered as a linear visco-elastic material. In addition to the heterogeneous cases, a homogeneous profile (i.e. $\alpha = 1$) has been investigated too. This has allowed to quantify the effect of the heterogeneity on the fundamental frequencies of the soil deposits and to compare the EERA results with the analytical solutions provided by Gazetas (1982).

Figure 5 shows the amplification functions obtained with EERA for the heterogeneous and homogeneous cases. The first two natural frequencies of the soil deposits are summarized in Table 2. Consistent with the literature (Gazetas 1982), two main phenomena can be recognized: with respect to the homogeneous case, the first natural frequency clearly shifts towards higher values as the parameter α increases, while the higher frequencies tend to reduce with increasing heterogeneity. The second frequency is higher than the one characterizing the homogeneous deposit only for α

Table 2. Natural frequencies of the soil profiles.

Soil profile	f_1 (Hz)	f_2 (Hz)
α _1	2.08	6.25
α _2.5	2.51	6.49
α _5	2.90	6.65
α _10	3.44	6.18
α _15	3.63	5.73

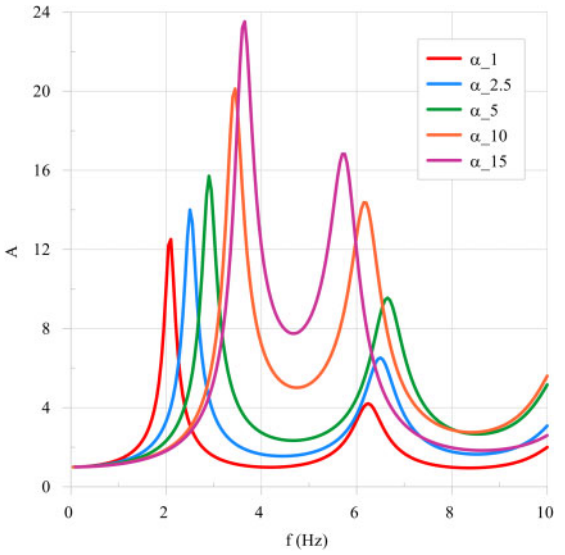

Figure 5. EERA amplification functions.

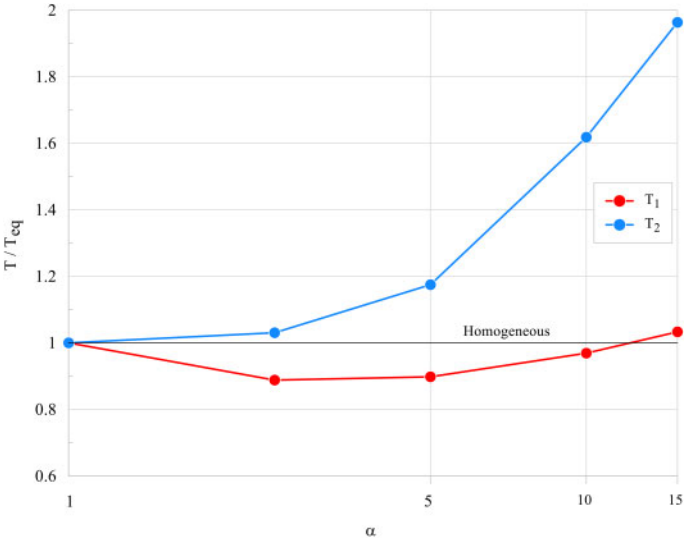

Figure 6. Normalized first and second soil natural periods as function of the heterogeneity parameter α.

equal to 2.5 and 5, but then reduces considerably for higher values of heterogeneity ratios. Secondly, the heterogeneity implies an evident amplification of all the natural frequencies, which can reach two or three times that observed for the homogeneous case. This can be attributed to the lower shear wave velocity adopted for the shallower soil layers as α increases.

Figure 6 presents the results of the EERA visco-elastic simulations in terms of first and second natural periods (T) of the heterogeneous deposits normalized by the "equivalent" homogeneous ones (T_{eq}). It should be noted that, according to Gazetas (1982), the equivalent homogeneous medium has been defined, for each of the four cases, as the one having the same shear wave velocity of the heterogeneous profile in the middle of the deposit. With this in mind, the figure shows that T_1 is lower than the first natural period of the equivalent homogeneous deposit, reaching

a minimum for $\alpha = 2.5$, and then becomes bigger for $\alpha = 15$. On the contrary, T_2 is always bigger than T_{eq} and seems to monotonically increase with the heterogeneity ratio.

3.2 *2D and 3D free-field analyses*

Having investigated with EERA the impact of the soil heterogeneity on the fundamental periods of the deposit under free-field conditions, the same problem has been replicated with ABAQUS using the previously described 2D and 3D models. The comparison between the EERA and the FE results is presented in Figure 7 in terms of amplification functions for the case of $\alpha = 2.5$. A very good agreement in the frequency range of interest (i.e. up to 10Hz) between both the 2D and 3D ABAQUS output and EERA can be recognized: the FE schemes catch very well the natural frequencies of the soil deposit and the peaks of the amplification function obtained through the visco-elastic approach, thus demonstrating the effectiveness of the Rayleigh damping calibration and the boundary conditions adopted in the FE simulations. Similar considerations can be drawn for the other deposits characterized by different heterogeneity ratios, not shown herein for the sake of brevity.

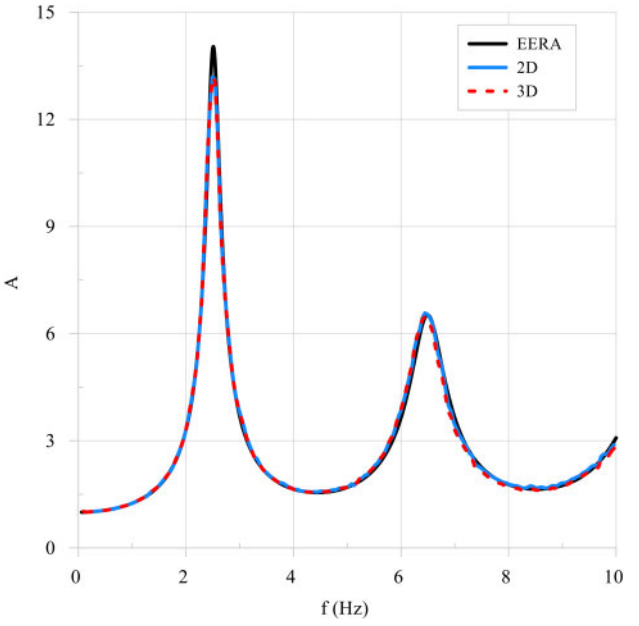

Figure 7. Comparison between EERA and ABAQUS amplification functions for $\alpha = 2.5$.

3.3 *3D soil-structure interaction analyses*

The tower, its foundation and the subsoil have been assembled in ABAQUS within a single 3D model (Figure 8a). The interface between the foundation and the visco-elastic deposit has been modeled by adopting a master-slave relationship: a penalty type interaction law has been defined for the tangential behaviour, while a hard contact type law has been imposed for the behaviour in the normal direction to prevent the interpenetration between the contact surfaces. A control point has been chosen on the top of the tower (point A), while other two points have been selected at foundation level (point B) and at the soil surface far enough from the structure (point C), representative of the free-field response, as shown in the cross section of the 3D model presented in Figure 8b.

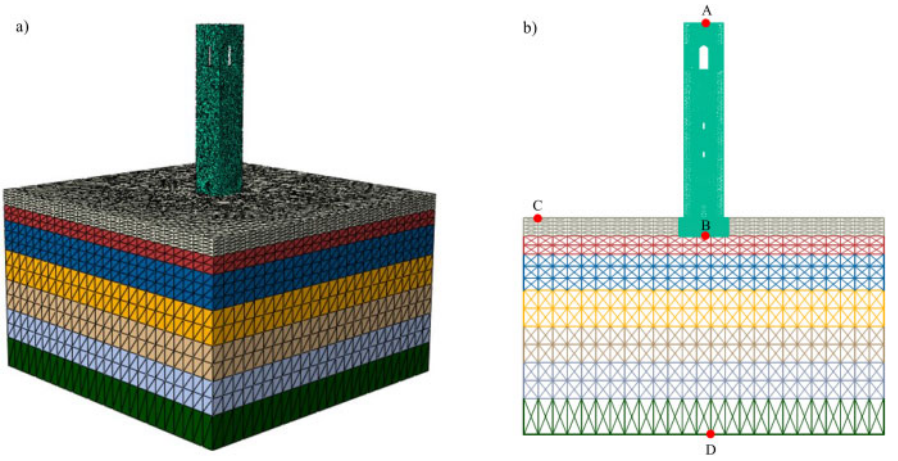

Figure 8. a) 3D SSI model and b) location of the control points.

In addition to the 3D models of the tower resting on class C deposits (with α equal to 1, 2.5, 5, 10 and 15), a further analysis has been performed with ABAQUS considering the structure standing on a very rigid homogeneous subsoil (assuming V_S=8000 m/s) to simulate the fixed-base condition. From this last simulation, the amplification function between point A and point C has allowed to identify the first two fundamental frequencies of the fixed-base tower, respectively equal to 1.81 and 8.25Hz, which are in agreement with a preliminary modal eigenvalue analysis.

The effects of SSI on the fundamental frequency and damping ratio of the system for different α values are shown in Figure 9, depicting the amplification functions between the tower motion recorded at the top (point A in Figure 8b) and the input motion applied at bedrock (point D in

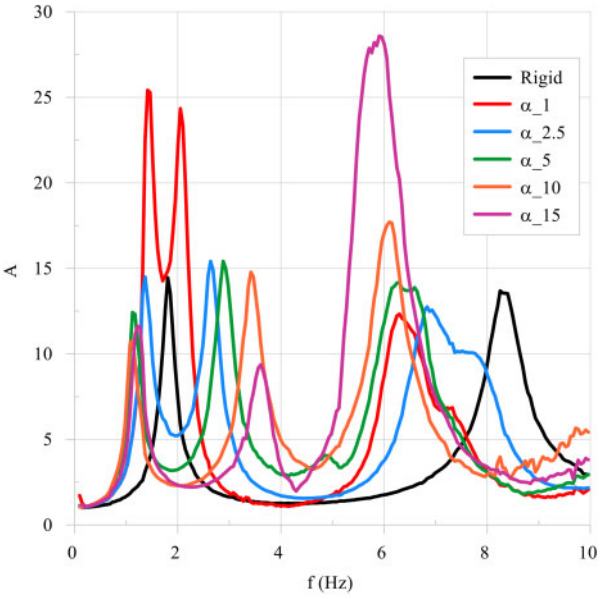

Figure 9. Amplification function of the full soil-structure system for different heterogeneity ratio α.

Figure 8b). The amplification function is used to identify the natural frequency of the soil-tower system, while its amplitude at the natural frequencies provides a measure of the damping ratio associated to the soil-tower system. It should be firstly noted that no relevant kinematic effects are expected in the case of a structure with a shallow foundation (Day 1978; Elsabee et al. 1977; Kim & Stewart 2003). Therefore, any deviation from a cantilever response of the tower can be essentially attributed to the inertial interaction between the structure and the soil deposit.

In Figure 9, each curve presents three distinct peaks which refer to the first three natural frequencies of the soil-structure system. The comparison with the rigid soil case, representing the fixed-base tower, helps to recognize the relative contribution given by the structure and the soil to the dynamic response of the full 3D model.

The first mode of vibration can be mainly attributed to the first flexural mode of the tower along the × direction, while the soil strongly affects the second and third mode since the natural frequencies of the system are practically coincident with the first and second natural mode of the deposit in free-field conditions.

The amplification functions between the tower motion recorded at the top (point A in Figure 8b) and the free-field response (point C in Figure 8b) give evidence to the typical effects of dynamic soil-structure interaction, as illustrated in Figure 10. Looking at the first (Figure 10a) and second (Figure 10b) mode of the tower, the primary effect of soil heterogeneity is to reduce the dynamic stiffness and increase the damping ratio of the soil-tower system, leading to smaller natural frequencies and lower magnitudes of the motion with respect to the cantilever condition. This effect is more pronounced for the higher soil heterogeneity ratios. In addition, much smaller values of the amplification factors are obtained when the second natural mode is inspected.

The reliability of the numerical approach has also been checked with reference to the analytical solution for single degree of freedom systems (SDOF) proposed by Veletsos & Nair (1975), looking at the first natural frequency in the homogeneous soil deposit case ($\alpha = 1$). The comparison has been carried out considering an equivalent SDOF oscillator characterized by a height (h) equal to the distance from the base to the centroid of mass of the structure (Veletsos & Nair 1975) and a concentrated mass equal to the whole mass of the tower. The foundation embedment effect has been estimated using the foundation impedance functions proposed by Gazetas (1991).

Figure 11 plots the ratio of the compliant base structure frequency (f_{SSI}) to the fixed-base one (f_0) as a function of the relative soil-structure stiffness parameter defined as follows:

$$\sigma = \frac{V_S}{f_0 h} \tag{4}$$

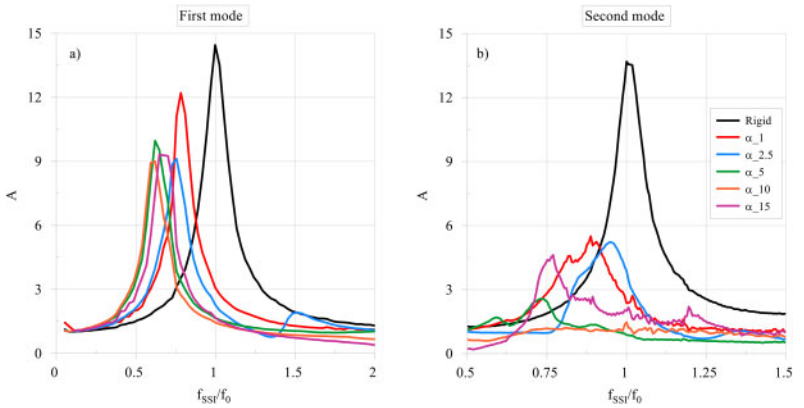

Figure 10. Amplification functions of the tower motion normalized a) by the first fixed-base frequency and b) by the second fixed-base frequency for different heterogeneity ratio α.

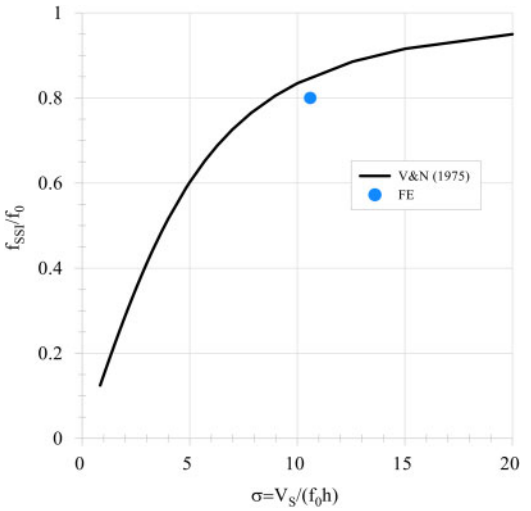

Figure 11. Comparison between the SSI FE result for the homogeneous soil deposit case (i.e. $\alpha = 1$) and the analytical solution proposed by Veletsos & Nair (1975).

The FE solution and the analytical value are in fair agreement considering all the assumptions made. In particular, the FE result tends to slightly overestimate (of about 5%) the frequency reduction related to SSI effects, with respect to the analytical solution.

Finally, the 3D FE results are plotted in terms of periods of the tower resting on the deformable soil (T_{SSI}) normalized by the fixed-base period (T_0) of the tower, as a function of the heterogeneity parameter α (Figure 12). The first natural period T_1 increases much more than the second one, T_2, for each considered heterogeneity ratio. In particular, starting from a value of about 1.28 for the homogeneous case, T_1 tends to increase for increasing values of the heterogeneity ratio, achieving its maximum value at $\alpha = 10$, beyond which the first period begins to decrease. The curve of

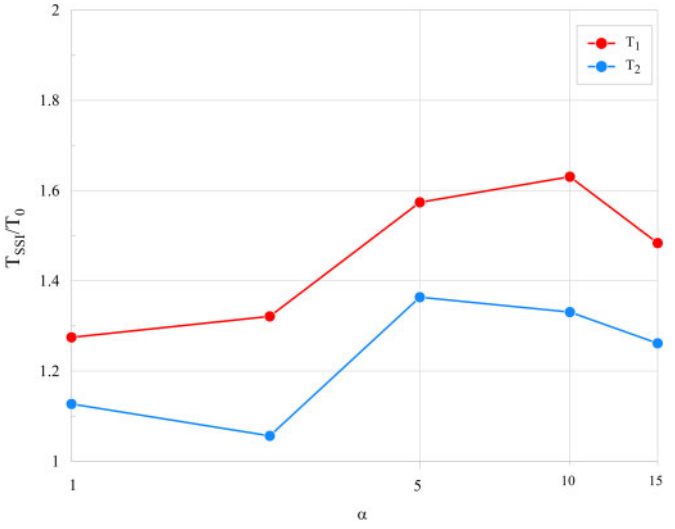

Figure 12. Normalized first and second tower T_{SSI} periods as function of the heterogeneity parameter α.

the normalized second oscillation period of the soil-tower system is instead characterized by an irregular trend, with T_2 varying between 1.13 and 1.36. The outputs suggest that the effects of the soil-structure interaction may be significant, with a change in the natural periods of the soil-tower system strongly dependent on the soil profile characteristics. These effects should be taken into account to obtain an accurate evaluation of the dynamic response of the system.

4 CONCLUSIONS

The paper deals with the assessment of the dynamic response of a typical masonry tower, specifically focusing on the effects of the soil deposit heterogeneity on the SSI phenomena. A set of four soil profiles, representative of real possible stratigraphies in Italy, has been considered, while the masonry tower exemplifies an ideal case study that sums up the main geometrical features of bell towers located in the seismic areas of Northern Italy. After a preliminary modelling, aimed at validating the numerical approach adopted for the seismic ground response of the subsoil foundation under free-field conditions, complete 3D dynamic SSI analyses have been performed to assess the modifications due to the soil heterogeneity of the soil-tower seismic behaviour with respect to the fixed-base condition, by considering a visco-elastic constitutive assumption for both the tower and its foundation deposits.

The numerical results show the typical effects related to soil-structure interaction, consisting in the period elongation of the structure and the increase of damping ratio with respect to the cantilever condition due to the soil deposit deformability, more pronounced for the first flexural mode rather than for the second one. Moreover, a clear coupling between the tower and the soil can be recognized for the second natural mode of the structure, which results to be more affected by the soil compliance than the first one.

The work presents only some preliminary results of the SSI problem affecting masonry towers on deformable soil deposits. Further developments of the ongoing research will account for the elasto-plastic behaviour of the tower, which could be described through a more sophisticated constitutive model, capable to predict the damage scenarios affecting the structure during representative earthquake motions.

REFERENCES

ABAQUS 2014. ABAQUS documentation version 6.14. Dassault Systèmes, Providence, RI.

Amorosi, A., Boldini, D., & Di Lernia, A. 2017. Dynamic soil-structure interaction: a three-dimensional numerical approach and its application to the Lotung case study. *Computers and Geotechnics*, 90, 34–54.

Amorosi, A., Boldini, D., & Elia, G. 2010. Parametric study on seismic ground response by finite element modelling. *Computers and Geotechnics*, 37(4), 515–528.

Bardet, J. P., Ichii, K., & Lin, C. H. 2000. EERA: a computer program for equivalent-linear earthquake site response analyses of layered soil deposits. University of Southern California, Department of Civil Engineering.

Bartoli, G., Betti, M., & Vignoli, A. 2016. A numerical study on seismic risk assessment of historic masonry towers: a case study in San Gimignano. *Bulletin of Earthquake Engineering*, 14(6), 1475–1518.

Bathe, K. J. 1996. *Finite element procedures in engineering analysis*, (2nd ed.) Upper Saddle River, NJ: Prentice Hall.

Casciati, S., & Borja, R. I. 2004. Dynamic FE analysis of South Memnon Colossus including 3D soil–foundation–structure interaction. *Computers and Structures*, 82(20–21), 1719–1736.

Casolo, S., Diana, V., & Uva, G. 2017. Influence of soil deformability on the seismic response of a masonry tower. *Bulletin of Earthquake Engineering*, 15(5), 1991–2014.

Casolo, S., & Uva, G. 2013. Non-linear dynamic analysis of masonry towers under natural accelerograms accounting for soil-structure interaction, *in: 4th ECCOMAS, Thematic Conference on Computational Methods in Structural Dynamics and Earthquake Engineering. Crete, Greece, 2013*, pp. 4488–4506.

Castellazzi, G., D'Altri, A. M., de Miranda, S., Chiozzi, A., & Tralli, A. 2018. Numerical insights on the seismic behaviour of a non-isolated historical masonry tower. *Bulletin of Earthquake Engineering*, 16(2), 933–961.

Clementi F., Milani G., Ferrante A., Valente M., & Lenci S. 2019. *Crumbling of Amatrice clock tower during 2016 Central Italy seismic sequence: Advanced numerical insights.* Frattura Ed Integrità Strutturale 14(51), 313–335.

Clough, R. W., & Penzien, J. 1993. *Dynamics of Structures*, McGraw-Hill.

Consiglio dei Ministri. 2018. DM 17 gennaio 2018 in materia di "aggiornamento delle norme tecniche per le costruzioni". Gazzetta ufficiale n.42 del 20 febbraio 2018.

Day SM. 1978. Seismic response of embedded foundations. *In Proceedings of the ASCE Convention, Chicago, IL, 16–20 October 1978*; Preprint no. 3450.

de Silva, F. 2020. Influence of soil-structure interaction on the site-specific seismic demand to masonry towers. *Soil Dynamics and Earthquake Engineering*, 131, 106023.

de Silva, F., Ceroni, F., Sica, S., & Silvestri, F. 2018a. Non-linear analysis of the Carmine bell tower under seismic actions accounting for soil–foundation–structure interaction. *Bulletin of Earthquake Engineering*, 16(7), 2775–2808.

de Silva, F., Pitilakis, D., Ceroni, F., Sica, S., & Silvestri, F. 2018b. Experimental and numerical dynamic identification of a historic masonry bell tower accounting for different types of interaction. *Soil Dynamics and Earthquake Engineering*, 109, 235–250.

di Lernia, A., Amorosi, A., & Boldini, D. 2019. A multi-directional numerical approach for the seismic ground response and dynamic soil-structure interaction analyses. *In Earthquake Geotechnical Engineering for Protection and Development of Environment and Constructions* (pp. 2145–2152). CRC Press.

Elsabee, F., Morray, J. P., & Roesset, J. M. 1977. *Dynamic behaviour of embedded foundations.* Massachusetts Institute of Technology, Department of Civil Engineering, Constructed Facilities Division.

Falcone, G., Acunzo, G., Mendicelli, A., Mori, F., Naso, G., Peronace, E., …& Moscatelli, M. 2021. Seismic amplification maps of Italy based on site-specific microzonation dataset and one-dimensional numerical approach. *Engineering Geology*, 289, 106170.

Gazetas, G. 1991. Formulas and charts for impedances of surface and embedded foundations. *Journal of Geotechnical Engineering*, 117(9), 1363–1381.

Gazetas, G. 1982. Vibrational characteristics of soil deposits with variable wave velocity. *International Journal for Numerical and Analytical Methods in Geomechanics*, 6(1), 1–20.

Kim, S., & Stewart, J. P. 2003. Kinematic soil-structure interaction from strong motion recordings. *Journal of Geotechnical and Geoenvironmental Engineering*, 129(4), 323–335.

Kuhlemeyer, R. L., & Lysmer, J. 1973. Finite element method accuracy for wave propagation problems. *Journal of the Soil Mechanics and Foundations Division*, 99(5), 421–427.

Milani, G. 2019. Fast vulnerability evaluation of masonry towers by means of an interactive and adaptive 3D kinematic limit analysis with pre-assigned failure mechanisms. *International Journal of Architectural Heritage*, 13(7), 941–962.

Mortezaei, A., & Motaghi, A. 2016. Seismic assessment of the world's tallest pure-brick tower including soil-structure interaction. *Journal of Performance of Constructed Facilities*, 30(5), 04016020.

Sarhosis, V., Milani, G., Formisano, A., & Fabbrocino, F. 2018. Evaluation of different approaches for the estimation of the seismic vulnerability of masonry towers. *Bulletin of Earthquake Engineering*, 16(3), 1511–1545.

Torabi, H., & Rayhani, M. T. 2014. Three-dimensional finite element modeling of seismic soil–structure interaction in soft soil. *Computers and Geotechnics*, 60, 9–19.

Valente, M., & Milani, G. 2018. Effects of geometrical features on the seismic response of historical masonry towers. *Journal of Earthquake Engineering*, 22(sup1), 2–34.

Valente, M., & Milani, G. 2016. Seismic assessment of historical masonry towers by means of simplified approaches and standard FEM. *Construction and Building Materials*, 108, 74–104.

Veletsos, A.S., & Nair, V.D. 1975. Seismic interaction of structures on hysteretic foundations. *Journal of the Structural Division*, 101, 109–29.